

Thermodynamic equilibrium calculations in cementitious systems

Barbara Lothenbach

Received: 22 October 2008 / Accepted: 5 April 2010 / Published online: 17 April 2010
© RILEM 2010

Abstract This review paper aims at giving an overview of the different applications of thermodynamic equilibrium calculations in cementitious systems. They can help us to understand on a chemical level the consequences of different factors such as cement composition, hydration, leaching, or temperature on the composition and the properties of a hydrated cementitious system. Equilibrium calculations have been used successfully to compute the stable phase assemblages based on the solution composition as well as to model the stable phase assemblage in completely hydrated cements and thus to assess the influence of the chemical composition on the hydrate assemblage. Thermodynamic calculations can also, in combination with a dissolution model, be used to follow the changes during hydration or, in combination with transport models, to calculate the interactions of cementitious systems with the environment. In all these quite different applications, thermodynamic equilibrium calculations have been a valuable addition to experimental studies deepening our understanding of the processes that govern cementitious systems and interpreting experimental observations. It should be carried in mind that precipitation and dissolution processes can

be slow so that thermodynamic equilibrium may not be reached; an approach that couples thermodynamics and kinetics would be preferable. However, as many of the kinetic data are not (yet) available, it is important to verify the results of thermodynamic calculations with appropriate experiments. Thermodynamic equilibrium calculations in its different forms have been applied mainly to Portland cement systems. The approach, however, is equally valid for blended systems or for cementitious systems based on supplementary cementitious materials and is expected to further the development of new cementitious materials and blends.

Keywords Thermodynamic modeling · Pore solution · Cements

1 Introduction

When Portland cement is brought into contact with water, its constituents start to react and various hydration products such as C-S-H (calcium silicate hydrate) gel, portlandite, ettringite, monosulfate or monocarbonate form. The composition of the cement, the interacting solution and the reaction time determine which solids (hydrates) will form, as the solid hydrates can precipitate only if the solutions are saturated or oversaturated with respect to the respective solid.

B. Lothenbach (✉)
Empa, Swiss Federal Laboratories for Materials Testing and Research, Laboratory for Concrete and Construction Chemistry, Überlandstrasse 129, 8600 Dübendorf, Switzerland
e-mail: barbara.lothenbach@empa.ch

The composition of hydrated cementitious systems can be quite complex. Thermodynamic modeling of such multicomponent–multiphase systems can promote our understanding of the impact of different factors such as composition, hydration, leaching, or temperature. In addition, adequate thermodynamic models allow easy and fast parameter variations and make it possible to predict the composition of hydrate assemblages under different conditions and to extrapolate it to longer time scales, possibly reducing the amount of long and costly experimentation.

Thermodynamic equilibrium calculations predict, based on generic data such as solubility products K_{SO} and complex formation constants of aqueous complexes, which complexes and solids are stable under the specific conditions of the experiment. Thermodynamic modeling is thus based on the knowledge of the thermodynamic data (e.g., solubility or complex formation) of all the solids, aqueous and gaseous species that can form in the system. These thermodynamic data are valid for all geochemical systems and compiled in different thermodynamic databases. Geochemical modeling codes (e.g., PHREEQC [1], MINEQL [2], EQ3/6 [3], CHESS [4], or GEMS [5, 6]) compute the equilibrium phase assemblage and speciation in a complex system from its total bulk elemental composition. Chemical interactions involving solids, solid solutions, gaseous phase and aqueous electrolytes are considered simultaneously.

Thermodynamic modeling can be used in cementitious systems to calculate the stable phase assemblages based on the solution composition [7–10], to model the influence of the composition of the stable phase assemblage [11–14], to model hydration [9, 15–18] or, often in combination with transport models, to calculate the interactions with the environment [19–24]. Since the early 1990s, thermodynamic modeling has been used to calculate the composition of hydrated Portland cements and to predict the composition of the solution in equilibria [25–35]. Thermodynamic calculations using the measured composition of the pore solution can also be used to identify which phase cannot form and which are potentially stable. The detailed knowledge of the composition of the pore solution can be used to predict the (potentially) stable solid as well as an instrument to verify thermodynamic modeling.

Even though the approach of thermodynamic modeling has not changed fundamentally, significant

progress has been made. More sophisticated geochemical softwares have been developed, the formation of solid solution models for various phases has been taken into account and, most importantly, the thermodynamic databases used became more adequate as the solubility products of more and more minerals present in cementitious systems were determined. While the use of different modeling software leads to very minor differences in the results [36], provided that the same database is used, the development of more adequate thermodynamic databases leads to more and more reliable thermodynamic calculations.

In some cases, however, thermodynamically stable phases may not form spontaneously or only very slowly. The formation of such phases (e.g., siliceous hydrogarnet, thaumasite) is generally suppressed in thermodynamic calculations to conform the observations. This introduces an element of expert knowledge or empirics into the else generic approach of thermodynamic modeling. Preferable would be an approach where thermodynamics and kinetics are considered simultaneously. Unfortunately many of the data which would enable us to couple thermodynamic with kinetics are still missing or incomplete.

This review paper gives short introduction to equilibrium calculations, an overview about the different thermodynamic databases available specifically for cementitious systems and about the changes in the pore solution during hydration. On these foundations, an overview of the different applications of thermodynamic modeling in cementitious systems and its possible uses in the investigation of cementitious materials is presented.

2 Thermodynamic equilibrium calculations

2.1 Approach

Thermodynamic equilibrium calculations predict the composition in a system composed of aqueous, solid and gaseous phases at the temperature and pressure of interest. Thermodynamic calculations, however, are more than just an easy tool for calculations. It allows testing different concepts and prevents us to make assumptions which violate mass conservations. The comparison with experimental data enables us to validate the calculations as well as the underlying assumptions.



Two basic approaches to solve the geochemical equilibrium problem are used in geochemical modelling codes: (i) solving the law of mass action (LAM) equations, or (ii) minimizing the Gibbs free energy of the system. The first approach is common and available in many speciation codes such as PHREEQC [1], MINEQL [2], EQ3/6 [3] or CHES [4] and extensively described in textbooks [37]. It requires $\log K$ values (see below) for the aqueous complexes, solids or gases at the temperature and pressure of interest. To calculate the composition of a system, mass and charge balances equations are solved iteratively using Newton–Raphson iterations.

The mass action constant of a reaction describes the equilibrium between different species. For the solubility product of gypsum, $\text{CaSO}_4 \cdot 2\text{H}_2\text{O}$, we might write:

$$K_{\text{SO}} = \frac{\{\text{SO}_4^{2-}\}\{\text{Ca}^{2+}\}\{\text{H}_2\text{O}\}^2}{\{\text{CaSO}_4 \cdot 2\text{H}_2\text{O}\}} = \{\text{SO}_4^{2-}\}\{\text{Ca}^{2+}\}\{\text{H}_2\text{O}\}^2 \quad (1)$$

where K is the equilibrium constant and $\{\}$ denotes the activity of the species. The activity of a pure solid phase such as gypsum in Eq. 1 is equal to one by definition. Activities of dissolved species (dimensionless) are related to molal concentrations $[\]$ (in mol/kg H_2O) by a correction term, the (dimensionless) activity coefficient, $\gamma : \{\text{Ca}^{2+}\} = \gamma_i \frac{[\text{Ca}^{2+}]}{[\text{Ca}^{2+0}]}$; $[\text{Ca}^{2+0}]$ is the molal concentration in the standard state and equals 1 mol/kg H_2O .

In addition to the effect of activity, the reactivity of ions in solution is reduced by the formation of aqueous complexes, e.g., CaOH^+ , CaSO_4^0 . The corresponding mass action constant is termed stability constant:

$$K_{\text{CaSO}_4^0} = \frac{\{\text{CaSO}_4^0\}}{\{\text{SO}_4^{2-}\}\{\text{Ca}^{2+}\}} \quad (2)$$

The Gibbs free energy minimisation approach is represented, e.g., by GEMS [5]. Thermodynamic equilibrium in a system is obtained when there is no spontaneous tendency for change anymore, i.e., at equilibrium the Gibbs free energy of the system is at a minimum. The Gibbs free energy of a system is defined as $G = \sum n_i \mu_i$, where n_i is the number of moles of the respective component and μ_i the partial molal Gibbs free energy. The GEM approach is based

on a mass and charge balance of the whole system. The equilibrium composition is calculated automatically from the stoichiometrically possible phases. Activity coefficients are calculated for each phase separately; several variable liquid and/or solid solutions might be considered.

The Gibbs free energy of reaction $\Delta_r G^\circ$ is related to the mass action constant according to:

$$\Delta_r G^\circ = \sum_i v_i \Delta_f G^\circ = -RT \ln K \quad (3)$$

where v_i are the stoichiometric coefficients of the reaction, $\Delta_f G^\circ$ the Gibbs free energy of formation of the individual compound, $R = 8.31451 \text{ J/mol/K}$ is the universal gas constant and T the temperature in Kelvin. For more detailed reading on thermodynamics and thermodynamic modeling of aqueous systems see geochemical text books [37–39].

Both approaches, the law of mass action (LMA) approach and the Gibbs free energy minimization approach, give comparable results [40]. While in many cases the LMA might be slightly faster with regard to calculation times, the Gibbs free energy minimization approach has the advantage that no a priori assumptions have to be made about the phases present, the compositions of solid solutions, pH, redox potential and the fugacity of gases but that these parameters are obtained as output parameters.

3 Influence of temperature and pressure

The thermodynamic properties both of a single species as well as of reactions depend on the temperature as well as on the pressure. Generally, tabulated thermodynamic data refer to the reference temperature T_0 of 298.15 K (25°C) and to the pressure of 1 bar (0.1 MPa).

Temperature corrections of reaction constants are often expressed with an equation of the form [38, 41]:

$$\log K_T = A_0 + A_1 T + \frac{A_2}{T} + A_3 \ln T + \frac{A_4}{T^2} + A_5 T^2 + A_6 \sqrt{T}, \quad (4)$$

where A_0, \dots, A_6 are constants. If the entropy (S°), the enthalpy ($\Delta_f H^\circ$) as well all the coefficients (a_0, a_1, \dots) of the heat capacity equation ($C_p^\circ = a_0 + a_1 T + a_2 T^{-2} + a_3 T^{-0.5} + \dots$) of the species are



available, the constants A_0, \dots, A_6 can be calculated directly (see [38, 41]), otherwise they can be fitted if sufficient experimental data are available.

Often the heat capacity of the reaction, $\Delta_r C_p^0$, is only known at reference temperature and is thus assumed to be constant in the considered temperature range. Then Eq. 4 can be reduced to the so called three-term approximation of the temperature dependence:

$$\log K_T = A_0 + \frac{A_2}{T} + A_3 \ln T \quad (5)$$

which gives a suitable approximation also for non-isoelectric reactions up to 150°C. The two-term extrapolation (Van't Hoff equation)

$$\log K_T = A_0 + \frac{A_2}{T} = \frac{0.4343}{R} \left(\Delta S_{T_0}^0 - \frac{\Delta H_{T_0}^0}{T} \right) \quad (6)$$

assumes that heat capacity of the reaction, $\Delta_r C_p^0$, equals zero and should be used only for isoelectric¹ or isocoulombic reactions. Examples for the influence of temperature on the solubility of different solids important for cementitious materials can be found, e.g., in [10, 42, 43].

Pressure corrections require that at least the change of volume $\Delta V_{T_0}^0$ of the reaction is known

$$\log K_{T,P} = \log K_T - \frac{0.4343}{RT} \Delta V_{T_0}^0 (P - P_0) \quad (7)$$

3.1 Activity corrections for aqueous species

The activity coefficients of dissolved ions or complexes account for the electrostatic shielding that occurs in the presence of a charged electrolyte and influences the reactivity of the ions. A number of different equations can be used to account for this effect. The most common equations used for thermodynamic modeling in cementitious systems are the Davies equation, which is considered to be valid for an ionic strength between 0.1 and 0.5 molal and the extended Debye–Hückel equation in the Truesdell–Jones form which is thought to be applicable up to 1–2 molal ionic strength [41].

$$\text{Davies : } \log \gamma_i = -A_\gamma z_i^2 \left(\frac{\sqrt{I_m}}{1 + \sqrt{I_m}} - 0.3I_m \right) \quad (8)$$

$$\begin{aligned} \text{Extended Debye – Hückel : } \log \gamma_i \\ = \frac{-A_\gamma z_i^2 \sqrt{I_m}}{1 + \dot{a} B_\gamma \sqrt{I_m}} + b_\gamma I_m \end{aligned} \quad (9)$$

where I_m is the effective molal ionic strength $I_m = \frac{1}{2} \sum m_i z_i^2$ in mol/kg H₂O, z_i the charge of the ion i , A_γ equals 0.51 and $B_\gamma = 0.33$ at 25°C and atmospheric pressure. \dot{a} and b_γ are parameters that have been individually evaluated for each ion by fitting the equation to measured activities of pure salt solutions [44] (both type of equations are used, e.g., in PHREEQC and GEMS). b_γ is a semi empirical coefficient, either individual for a given electrolyte [44] or common for all minor species in the predominant electrolyte (i.e. $b_\gamma = 0.064$ in NaCl electrolyte [45]). At ionic strength >1 molal the use of SIT (specific ion interaction term [46]) or the Pitzer approach [47] is required.

3.2 Uptake of ions

Many ions may become also sorbed on the surfaces of solids built into the structure of solids. One may distinguish surface complexation reactions (the formation of coordinative bonds at the surface) and ion exchange reactions based on electric interactions, which extend over larger distances. Formally this kind of reaction constants are treated like other mass action constants (see above). The uptake of different cations and anions by C-S-H has been described as surface complexation reaction [48–53] or based on surface charge [54].

The structural incorporation of ions in solid phases may be described in terms of solid solutions. Solid solutions are frequently encountered in cementitious systems [43, 55–58]. A solid solution is a homogeneous crystalline structure in which one or more types of atoms or molecules are partly substituted without changing the structure, although the lattice parameters may vary [59]. If the size and crystal lattice between host and substituting ion are similar, the formation of an ideal solid solution is probable. The larger the difference, the stronger is the tendency to non-ideality [59, 60] and thus the tendency for the presence of miscibility gaps. The presence of ideal or

¹ An isoelectric reaction exhibits equal charges on both sides such as $\text{Ca}^{2+} + \text{H}_2\text{O} \leftrightarrow \text{CaOH}^+ + \text{OH}^+$, while an isocoulombic reaction is a reaction with identically charged species on either side (e.g., $\text{Cl}^- + \text{H}_2\text{O} \leftrightarrow \text{HCl} + \text{OH}^-$).



non-ideal solid solutions can stabilize the formation of these solids and may result in a significant deviation of dissolved ion concentrations. Details on the thermodynamics of solid solutions can be found in the excellent books of Bruno et al. [59] or Anderson and Crerar [38].

4 Thermodynamic databases

Thermodynamic equilibrium modeling is based on the knowledge of the thermodynamic data (e.g., solubility products, complex formation constants) of all the solids, aqueous and gaseous species that can form in the system. The quality of the results of thermodynamic modeling depends directly on the quality and the completeness of the underlying thermodynamic database.

Thermodynamic data for complexes and solids generally present in geochemical systems, such as gypsum or calcite, have been critically reviewed and can be found in a number of compilations (e.g., [61–67]). Specific thermodynamic data for cementitious systems, such as the solubility products of ettringite or hydrogarnet, are generally not included in such generic databases but are compiled separately in “specific” databases for cementitious systems. It should be noticed that such specific databases have been always developed as supplemental to an existing database and thus can be used only together with the respective database.

4.1 Databases for cementitious systems

Several thermodynamic databases for cement minerals have been compiled and published. The first compilation was published as early as 1965 by Babushkin et al. [62, 68]. A number of other databases focusing on the solubility of cementitious materials based on the latest experimental data (at the time of publishing), have appeared in the meantime, e.g., [15, 17, 27, 31, 33, 34, 69–71]. The most recent cement specific cement database [10, 43] was published in 2007/2008 and contains thermodynamic data (solubility product, Gibbs free energy, enthalpy, entropy, heat capacity and molecular volume) for a number of cement phases. Solubility data have been generally calculated based on a critical review of the available experimental data and on additional

experiments to derive missing data or to verify the existing data. In addition, some data were estimated based on structural analogues. The data collection and selection is documented in different papers [10, 17, 43, 72]. Where necessary, additional solubility data were measured in a range of temperatures between 0 and 100°C [43, 58, 73]. The resulting data base Cemdata 2007 (see Table 1) covers hydrates commonly encountered in Portland cement systems in the temperature range 0–100°C, including C-S-H, hydrogarnet, hydrotalcite, AFm and AFt phases and their solid solutions.

Alkalis are taken up by the C-S-H phase. Low Ca/Si ratios as well as the presence of aluminum increase the uptake of alkalis [74–76]. Often empirical relations between the total amount of alkalis, the quantity of C-S-H and of the pore solution have been used to model the uptake of alkali by C-S-H [75–78]. The uptake of different cations and anions has also been described in terms of surface complexation [48–53], surface charge [54] or in the framework of a solid solution between C-S-H and alkali silicate hydrates [79].

4.2 Gaps in existing cement databases

Even though more and more thermodynamic data have become available in the last few years, several important gaps still exist in the different thermodynamic databases covering cementitious systems:

- Not only potassium and sodium, but also many other ions including aluminum, iron, chloride, sulfate or carbonate can be taken up by the C-S-H phase. Low Ca/Si, as present in blended or alkali activated slag or fly ash systems, increase the uptake of Al in C-S-H [80] and decrease the uptake of sulfate [81]. Further systematic experimental data on the uptake of different cations and anions as well as on their reciprocal influence are needed to improve our knowledge on the fate of these ions in hydrated cements
- The Al-containing phases ettringite, monosulfate and monocarbonate, together with hydrotalcite, determine the fate of aluminium in Portland cements. The fate of Fe during hydration, however, is controversial. The formation of Fe-ettringite, Fe-monosulfate, Fe-monocarbonate, Fe(OH)₃ or Fe-containing siliceous hydrogarnet from their

Table 1 Solubility constants used for the equilibrium calculations

Mineral	log K_{S0}	Dissolution reactions used to calculate solubility products log K_{S0}
Ettringite	−44.9	$\text{Ca}_6\text{Al}_2(\text{SO}_4)_3(\text{OH})_{12}\cdot 26\text{H}_2\text{O} \leftrightarrow 6\text{Ca}^{2+} + 2\text{Al}(\text{OH})_4^- + 3\text{SO}_4^{2-} + 4\text{OH}^- + 26\text{H}_2\text{O}$
Tricarboaluminate	−46.5	$\text{Ca}_6\text{Al}_2(\text{CO}_3)_3(\text{OH})_{12}\cdot 26\text{H}_2\text{O} \leftrightarrow 6\text{Ca}^{2+} + 2\text{Al}(\text{OH})_4^- + 3\text{CO}_3^{2-} + 4\text{OH}^- + 26\text{H}_2\text{O}$
Fe-ettringite	−44.0	$\text{Ca}_6\text{Fe}_2(\text{SO}_4)_3(\text{OH})_{12}\cdot 26\text{H}_2\text{O} \leftrightarrow 6\text{Ca}^{2+} + 2\text{Fe}(\text{OH})_4^- + 3\text{SO}_4^{2-} + 4\text{OH}^- + 26\text{H}_2\text{O}$
Thaumasite	−49.4	$\text{Ca}_6(\text{SiO}_3)_2(\text{SO}_4)_2(\text{CO}_3)_2\cdot 30\text{H}_2\text{O} \leftrightarrow 6\text{Ca}^{2+} + 2\text{H}_3\text{SiO}_4^- + 2\text{SO}_4^{2-} + 2\text{CO}_3^{2-} + 2\text{OH}^- + 26\text{H}_2\text{O}$
C_3AH_6	−20.84	$\text{Ca}_3\text{Al}_2(\text{OH})_{12} \leftrightarrow 3\text{Ca}^{2+} + 2\text{Al}(\text{OH})_4^- + 4\text{OH}^-$
Siliceous hydrogarnet	−29.87	$\text{Ca}_3\text{Al}_2(\text{SiO}_4)_{0.8}(\text{OH})_{8.8} \leftrightarrow 3\text{Ca}^{2+} + 2\text{Al}(\text{OH})_4^- + 0.8\text{SiO}(\text{OH})_3^- + 3.2\text{OH}^- - 2.4\text{H}_2\text{O}$
C_3FH_6	−25.16	$\text{Ca}_3\text{Fe}_2(\text{OH})_{12} \leftrightarrow 3\text{Ca}^{2+} + 2\text{Fe}(\text{OH})_4^- + 4\text{OH}^-$
C_4AH_{13}	−25.40	$\text{Ca}_4\text{Al}_2(\text{OH})_{14}\cdot 6\text{H}_2\text{O} \leftrightarrow 4\text{Ca}^{2+} + 2\text{Al}(\text{OH})_4^- + 6\text{OH}^- + 6\text{H}_2\text{O}$
C_2AH_8	−13.56	$\text{Ca}_2\text{Al}_2(\text{OH})_{10}\cdot 3\text{H}_2\text{O} \leftrightarrow 2\text{Ca}^{2+} + 2\text{Al}(\text{OH})_4^- + 2\text{OH}^- + 3\text{H}_2\text{O}$
Monosulfoaluminate	−29.26	$\text{Ca}_4\text{Al}_2(\text{SO}_4)(\text{OH})_{12}\cdot 6\text{H}_2\text{O} \leftrightarrow 4\text{Ca}^{2+} + 2\text{Al}(\text{OH})_4^- + \text{SO}_4^{2-} + 4\text{OH}^- + 6\text{H}_2\text{O}$
Monocarboaluminate	−31.47	$\text{Ca}_4\text{Al}_2(\text{CO}_3)(\text{OH})_{12}\cdot 5\text{H}_2\text{O} \leftrightarrow 4\text{Ca}^{2+} + 2\text{Al}(\text{OH})_4^- + \text{CO}_3^{2-} + 4\text{OH}^- + 5\text{H}_2\text{O}$
Hemicarboaluminate	−29.13	$\text{Ca}_4\text{Al}_2(\text{CO}_3)_{0.5}(\text{OH})_{13}\cdot 5.5\text{H}_2\text{O} \leftrightarrow 4\text{Ca}^{2+} + 2\text{Al}(\text{OH})_4^- + 0.5\text{CO}_3^{2-} + 5\text{OH}^- + 5.5\text{H}_2\text{O}$
Strätlingite	−19.70	$\text{Ca}_2\text{Al}_2\text{SiO}_2(\text{OH})_{10}\cdot 3\text{H}_2\text{O} \leftrightarrow 2\text{Ca}^{2+} + 2\text{Al}(\text{OH})_4^- + 1\text{SiO}(\text{OH})_3^- + \text{OH}^- + 2\text{H}_2\text{O}$
C_4FH_{13}	−29.4*	$\text{Ca}_4\text{Fe}_2(\text{OH})_{14}\cdot 6\text{H}_2\text{O} \leftrightarrow 4\text{Ca}^{2+} + 2\text{Fe}(\text{OH})_4^- + 6\text{OH}^- + 6\text{H}_2\text{O}$
C_2FH_8	−17.6*	$\text{Ca}_2\text{Fe}_2(\text{OH})_{10}\cdot 3\text{H}_2\text{O} \leftrightarrow 2\text{Ca}^{2+} + 2\text{Fe}(\text{OH})_4^- + 2\text{OH}^- + 3\text{H}_2\text{O}$
Fe-monosulfate	−33.2	$\text{Ca}_4\text{Fe}_2(\text{SO}_4)(\text{OH})_{12}\cdot 6\text{H}_2\text{O} \leftrightarrow 4\text{Ca}^{2+} + 2\text{Fe}(\text{OH})_4^- + \text{SO}_4^{2-} + 4\text{OH}^- + 6\text{H}_2\text{O}$
Fe-monocarbonate	−35.5*	$\text{Ca}_4\text{Fe}_2(\text{CO}_3)(\text{OH})_{12}\cdot 5\text{H}_2\text{O} \leftrightarrow 4\text{Ca}^{2+} + 2\text{Fe}(\text{OH})_4^- + \text{CO}_3^{2-} + 4\text{OH}^- + 5\text{H}_2\text{O}$
Fe-hemcarbonate	−33.1*	$\text{Ca}_4\text{Fe}_2(\text{CO}_3)_{0.5}(\text{OH})_{13}\cdot 5.5\text{H}_2\text{O} \leftrightarrow 4\text{Ca}^{2+} + 2\text{Fe}(\text{OH})_4^- + 0.5\text{CO}_3^{2-} + 5\text{OH}^- + 5.5\text{H}_2\text{O}$
Fe-strätlingite	−23.7*	$\text{Ca}_2\text{Fe}_2\text{SiO}_2(\text{OH})_{10}\cdot 3\text{H}_2\text{O} \leftrightarrow 2\text{Ca}^{2+} + 2\text{Fe}(\text{OH})_4^- + 1\text{SiO}(\text{OH})_3^- + \text{OH}^- + 2\text{H}_2\text{O}$
CAH_{10}	−7.5	$\text{CaAl}_2(\text{OH})_8\cdot 6\text{H}_2\text{O} \leftrightarrow \text{Ca}^{2+} + 2\text{Al}(\text{OH})_4^- + 6\text{H}_2\text{O}$
M_4AH_{10}	−56.02*	$\text{M}_4\text{Al}_2(\text{OH})_{14}\cdot 3\text{H}_2\text{O} \leftrightarrow 4\text{Mg}^{2+} + 2\text{Al}(\text{OH})_4^- + 6\text{OH}^- + 3\text{H}_2\text{O}$
M_4ACH_9	−51.14*	$\text{M}_4\text{Al}_2(\text{OH})_{12}\text{CO}_3\cdot 3\text{H}_2\text{O} \leftrightarrow 4\text{Mg}^{2+} + 2\text{Al}(\text{OH})_4^- + \text{CO}_3^{2-} + 4\text{OH}^- + 3\text{H}_2\text{O}$
M_4FH_{10}	−60.0*	$\text{M}_4\text{Fe}_2(\text{OH})_{14}\cdot 3\text{H}_2\text{O} \leftrightarrow 4\text{Mg}^{2+} + 2\text{Fe}(\text{OH})_4^- + 6\text{OH}^- + 3\text{H}_2\text{O}$
Jennite-type C-S-H	−13.17	$(\text{CaO})_{1.6667}(\text{SiO}_2)(\text{H}_2\text{O})_{2.1} \leftrightarrow 1.6667\text{Ca}^{2+} + \text{SiO}(\text{OH})_3^- + 2.3333\text{OH}^- - 0.5667\text{H}_2\text{O}$
Tobermorite-type C-S-H	−8.0	$(\text{CaO})_{0.8333}(\text{SiO}_2)(\text{H}_2\text{O})_{1.3333} \leftrightarrow 0.8333\text{Ca}^{2+} + \text{SiO}(\text{OH})_3^- + 0.6667\text{OH}^- - 0.5\text{H}_2\text{O}$
$\text{SiO}_{2,\text{am}}$	1.476	$\text{SiO}_{2,\text{am}} \leftrightarrow \text{SiO}(\text{OH})_3^- - 1\text{OH}^- - 1\text{H}_2\text{O}$
Syngenite	−7.2	$\text{K}_2\text{Ca}(\text{SO}_4)_2\text{H}_2\text{O} \leftrightarrow 2\text{K}^+ + 1\text{Ca}^{2+} + 2\text{SO}_4^{2-} + 1\text{H}_2\text{O}$
$\text{Al}(\text{OH})_{3,\text{am}}$	0.24	$\text{Al}(\text{OH})_{3,\text{am}} \leftrightarrow \text{Al}(\text{OH})_4^- - 1\text{OH}^-$
$\text{Fe}(\text{OH})_{3,\text{mic}}$	−4.60	$\text{Fe}(\text{OH})_{3,\text{am}} \leftrightarrow \text{Fe}(\text{OH})_4^- - 1\text{OH}^-$

All data were critically evaluated and compiled in [10, 43, 72]

* Tentative values

constitutive components have been observed [73, 82]. In cementitious systems, however, the situation seems to be more complex. For example, the formation of Fe-containing siliceous hydrogarnet in cementitious systems was reported in several studies [83–85], while others indicated the formation of amorphous Fe-hydroxides or of mixed Al–Fe-hydrates (cf. Taylor [86] and references therein). Recently, the solubility of Fe-ettringite, Fe-monosulfate and Fe-monocarbonate was determined experimentally [73]. For other hydrates such as Fe-containing hydrotalcites, siliceous

hydrogarnets and hydrogarnets, however, only rough estimates of the solubility data are presently available [10, 62]. These estimates require verification of the solubility of the above solids under well-controlled experimental conditions.

- Hydrotalcites have a variable composition of the general formula $\text{Mg}_{1-x}(\text{Al},\text{Fe})_x(\text{OH})_2\cdot[\text{A}^{n-}]_{x/n}\cdot m\text{H}_2\text{O}$, and a structure composed of positively charged brucite-like layers intercalated with anions $[\text{A}^{n-}]$ and water molecules. The structure can accommodate a number of cations including Mn, Mg, Ni, Zn, Al, Fe, interlayer anions such as



OH^- , Cl^- , CO_3^{2-} and SO_4^{2-} and a varying amount of water. Thermodynamic data for hydrotalcite are scarce due to its wide compositional variation, even though some thermodynamic data have been determined [30, 31, 87, 88]. The elemental composition of hydrotalcites does affect the distribution of aluminum and iron in cements and thus the quantity of AFm and AFt formed.

4.3 Kinetic restrictions

By applying thermodynamic modeling to cementitious systems, one implicitly assumes that a constrained thermodynamic equilibrium is present, i.e., that the liquid (pore solution) and the solid phase (hydrates) are in equilibrium. Most precipitation and dissolution processes are sufficiently fast so that the assumption of a thermodynamic equilibrium can be justified. Prominent exceptions are the dissolution of the clinker phases, which depends on the composition of the solution and can be slow under the conditions present in Portland cements, and the precipitation of some phases, e.g., hydrogarnets.

It has been observed that a number of factors influence the dissolution kinetics of the clinker phases; C_3S dissolution is strongly affected by the presence of pH and the Ca concentration (e.g., [89–92]) while high sulfate concentrations slow down C_3A dissolution [93]. Further factors influencing the dissolution of clinkers are impurities and the presence of defects in its structure [94]. Even though the influence of some parameters has been studied, there are still many parameters missing which are needed to develop a reliable model for the dissolution of Portland cements taking fully into account the composition of the surrounding solution. Thus, often alternative approaches are used which describe the dissolution of clinker phases using microstructural models [95] or purely empirical models [9, 77, 96], which up to now still neglect the influence of chemistry on the dissolution kinetics.

Even though pore solutions are generally slightly oversaturated with respect to the hydrates forming (Fig. 2), the system is close to thermodynamic equilibrium so that the assumption of equilibrium conditions seems to be a valid approach. In some cases, however, thermodynamically stable phases may not form spontaneously or only very slowly. C-S-H is metastable with respect to crystalline phases

but this condition is generally suspended in thermodynamic calculations to conform the observations. Hydrogarnets (C_3AH_6) have been observed to form only after weeks to months in solutions containing Al and Ca [97, 98]. Siliceous hydrogarnets ($\text{C}_3\text{AS}_x\text{H}_{6-2x}$; $x \leq 1$) have been synthesized around 100°C [43, 99], but do seem to form at ambient temperatures only very slowly. Hydrothermally prepared siliceous hydrogarnets are thermodynamically more stable than monosulfates or monocarbonates at ambient temperature and should thus replace AFm phases in cementitious systems. Numerous studies, however, reported the presence of monosulfate or monocarbonate in hydrated Portland cement systems, while no or only traces of siliceous hydrogarnets, which can contain aluminum and/or iron, have been detected in Portland cements hydrated at ambient temperatures [9, 100]. On the other hand, in Portland cements hydrated at 80°C or higher, significant quantities of siliceous hydrogarnets have been observed [10, 84]. Thus, even though siliceous hydrogarnets are thermodynamically stable at ambient temperatures, their presence is hardly observed probably due to their slow kinetics of formation. Therefore, in thermodynamic calculations the formation of siliceous hydrogarnets is often suppressed.

The suppression of certain phases, which do not form at ambient temperatures, by the user of thermodynamic models, introduces an element of expert knowledge or empirics into the otherwise generic approach of thermodynamic modeling. This can potentially lead to biased results. An approach that couples thermodynamics with kinetics would be preferable. The kinetic of precipitation (or dissolution) of a solid depends on number of parameters such as the degree of over- (or under-)saturation, the presence of surface defects such as kink, steps or pits, the composition of the solution, diffusion phenomena, the presence of other ions which hinder the reaction, pH and temperature [37, 39, 101, 102]. For a number of minerals, e.g., calcite [101, 103, 104] or gypsum [105, 106] many of the parameters influencing the dissolution/precipitation processes have been investigated and corresponding models have been formulated to couple thermodynamic with kinetic. Unfortunately, generally such data are not available for the high pH conditions relevant for cement systems. A very few authors also investigated under conditions relevant for cementitious systems the influence of the composition



of the aqueous phase on the precipitation kinetics; such studies are available for ettringite and calcium aluminate hydrates [107–110].

5 Pore solutions

The composition of the aqueous phase of hydrating cement can give important insights into the chemical processes and the interactions between solid and liquid phases. The composition of the liquid phase determines which hydrate phases are stable and can thus (potentially) precipitate. The measured composition of the pore solution and its changes during hydration can be considered in many cases as a prerequisite for a good thermodynamic model.

The following extensive discussion on how pore solutions can be obtained, on the composition of the pore solutions in different cementitious systems as well as on the question whether the expression with the pressure device will significantly change its composition, is the basis for many applications of thermodynamic equilibrium calculations. The findings of the composition of the pore solutions will be used in Sect. 6.1 to discuss the different uses of thermodynamic modeling.

Pore solutions can be collected during the first hours of hydration by vacuum filtration or centrifugation [111–113]. After hardening, pore solution can either be gained from samples where extremely high w/c ratio were employed [114–118] or by using a high pressure device to extract the pore solutions. Longuet et al. [119] were the first to describe such a high pressure device to extract pore solutions from hardened cement pastes. After the publications of Barneyback and Diamond [120, 121], who modified the device to be suitable also for mortars, the expression of liquids from cement pore solutions became quite popular. In a number of different studies [7–9, 17, 100, 111, 114, 117, 119, 121–126] the basic behavior of Al, Ca, K, Na, Si, sulfate and hydroxide concentrations during the hydration of Portland cement has been established.

5.1 Pore solution during the hydration of Portland cement

During the first hours the composition of pore solution of Portland cement is dominated by

potassium, sodium, sulfate, hydroxide and calcium (cf. Fig. 1). The high concentrations of potassium, sodium and sulfate observed after only a few minutes are due to the fast dissolution of alkali sulfate phases. The concentrations of calcium sulfate and hydroxide remain more or less constant during the first hours as their concentrations are limited by the presence of gypsum ($\text{CaSO}_4 \cdot 2\text{H}_2\text{O}$) or anhydrite (CaSO_4) and portlandite ($\text{Ca}(\text{OH})_2$). The concentrations of Al, Fe and Si (the oxides of these elements constitute together approx. 30 wt% of an ordinary Portland cement) in the pore solution are always very low.

A significant change in the composition of the pore solution is observed between 6 and 24 h (Fig. 1); calcium and sulfate concentrations decrease as solid gypsum and anhydrite are depleted due to the formation of ettringite, while hydroxide concentrations increase at the same time.

The observed trends in K, Na, Ca, S, Si, Al and OH^- concentrations as given in Fig. 1 are consistent with those reported in different studies [7, 9, 100, 114, 119, 122, 125, 127]. In general, the early Ca and Si concentrations reported in these investigations are similar, while the K, Na, initial S and OH^- concentrations strongly depend on the composition of the cement and the w/c ratio used in the different studies. After a hydration of one day and longer, the pore solution of Portland cements with high alkali contents exhibit high K and Na concentrations, thus also high OH^- and relatively low Ca concentrations. The Ca concentration in Portland cement systems is

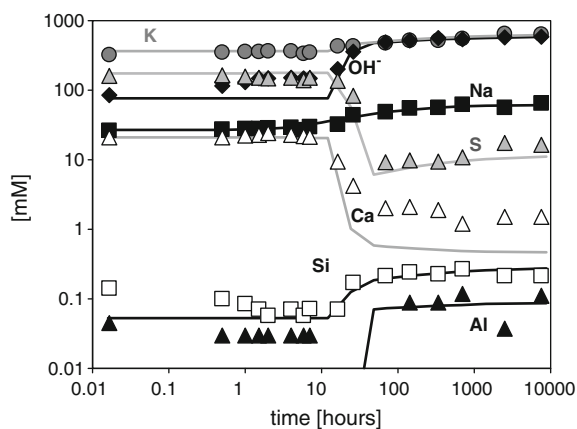


Fig. 1 Evolution of the pore solution during the hydration of OPC. Symbols refer to measured concentrations, lines to modeled concentrations. Adapted from [17]

determined by the solubility of portlandite and increases with decreasing pH or OH^- concentration. In addition, higher pH values also give rise to higher sulfate, Si, Al and Fe concentrations [7–9, 17, 100, 118, 123, 124].

5.2 Influence of temperature

The temperature during hydration influences not only the kinetics of hydration but also the composition of the pore solutions [125, 126, 128]. In the temperature range 5–50°C, the same changes in the composition of the pore solution are observed, but these changes occur much faster at 50°C than at 5°C as at higher temperatures the reactions are accelerated. After 7 days and longer, most elements in the pore solution show similar concentrations between 5 and 50°C with the exception of sulfate, aluminum and iron [125, 126, 128]. Sulfate concentrations are increased at 50°C, while the Al and Fe concentrations are lower. Higher temperatures result in more rapid reactions and temperature influences also the solubility products. The solubility of ettringite increases strongly with increasing temperature [42], while the increase of solubility of monosulfate is much less distinct [43]. Thus, the sulfate concentrations increase with temperature, until around 48°C ettringite becomes less stable than monosulfate [10, 129] in OPC systems. In contrast to sulfate, the concentrations of calcium and aluminum, which are restricted also by portlandite and monocarbonate, remain relatively constant in OPC systems.

5.3 Other systems

The blending of OPC with supplementary cementitious materials rich in silicon and poor in alkalis leads to a reduction of the pH and the alkali concentrations in the pore solutions as (i) the Portland cement is diluted and (ii) as C-S-H with a lower C/S ratio leads to an increase in alkali uptake by C-S-H [75, 76].

The blending of Portland cement with low calcium fly ash lowers the alkali and hydroxide concentrations in the pore solution significantly [121, 124, 130–133]. The same effect can also be observed for Portland systems blended with silica fume [133–135]. In contrast, the addition of metakaolin was observed to increase the pH of the pore solution [136]. High calcium fly-ash systems have been observed to

exhibit pH values in the range of 12–13, relatively low alkali concentration but higher aluminum concentrations than Portland cement systems [137].

In Portland cements blended with slags, lower pH values have been observed as well as the presence of reducing conditions [116, 119, 130, 135, 138], which is mirrored in high concentrations of reduced sulfur species such as sulfide (HS^-), sulfite (SO_3^{2-}) and thiosulfate ($\text{S}_2\text{O}_3^{2-}$) in the pore solutions. In slag-containing systems, the pH values are not only determined by the amount of dissolved alkalis, but also by the presence of high concentrations of negatively charged soluble sulfur species, which lower the hydroxide concentrations in the pore solution significantly.

Super sulfated slag cements exhibit, similar to slags blended with Portland cement, somewhat lower pH values than Portland cements [139, 140], while alkali activated slag systems are characterized by their high pH values [141–143]. An increase of the amount of alkaline activator increases not only the alkali concentrations and pH values but also Al and Si concentrations and decreases the Ca concentrations [141, 142, 144].

In calcium aluminate cements, the dissolved calcium and aluminum concentrations in the pore solutions increase quickly to a maximum with a Ca/Al molar ratio around 1.1. Eventually solids start to precipitate and the concentrations fall rapidly [70, 107–109, 145]. The pore solution of calcium sulfoaluminate cements exhibit relatively high aluminum concentrations of approx. 10 mM and initially a pH of 10–11, which increases once the calcium sulfate is consumed to 12.5–13 [146, 147].

5.4 Representativity of pore solutions obtained at high pressures

It has been argued that the solution expressed using a pressure device may not represent the real pore solution present in the hydrating cements [148]. Even though relatively high w/c ratios (0.4–0.6) are generally used in pore solution experiments (to ensure that some pore solution can be squeezed out), high pressures might need to be applied to the solid samples. In that case, an increase of pressure could affect the composition of the solution pressed out. For pore solutions gained from OPC and OPC blended with slag or fly ash prepared with a w/c of 0.5 [149]

and 0.6 [150], no significant influence of the pressure used (up to 560 and 350 MPa, respectively) on the alkali, hydroxide and chloride concentrations was observed. Pore solutions from OPC samples (w/c 0.42) expelled at pressures up to 1,000 MPa, however, showed at higher pressures an increase in alkali concentrations of 20–30% [151], while pore solutions using pressures between 60 and 330 MPa (OPC, w/c = 0.4) showed a slight increase in Na, K, Na and OH⁻ concentration in the range of 4–9% (Table 2); a difference that is in the range of the variability of pore solution extraction data [150]. For silicon a slight increase of the concentrations with pressure is observed. For sulfate, however, a clear increase of the measured concentrations with increasing pressure is found.

These data (Table 2; [149–151]) indicate that the concentrations expelled with pressures up to approx. 500 MPa are comparable to each other, even though concentrations increase somewhat with the pressure applied. At higher pressures, however, the composition will start to differ significantly. The high pressures applied to expel the pore solutions could be the cause of this concentration increase, as high pressures could increase the solubility of solids.

6 Thermodynamic modeling

The thermodynamic modeling of cement systems can enable us to understand on a chemical level the consequences of different factors such as cement composition, hydration, leaching, or temperature on the composition and the properties of a hydrated cementitious system. Thermodynamic modeling has

been used in cementitious systems (i) for the calculation of the stable phase assemblages based on the solution composition, (ii) to model the influence of the initial composition on the finally resulting stable phase assemblage, (iii) to model the changes associated with hydration or (iv), often in combination with transport models, to calculate the interactions with the environment.

6.1 Calculation of hydrate assemblage based on the composition of the pore solution

During the hydration solid hydrates are formed in contact with the surrounding pore solution. The composition of the pore solution can thus provide information about the stability of hydration products. Comparing the ion activity product (IAP) of a solid with its equilibrium solubility product (K_{SO}) gives the degree of over- or undersaturation and thus information whether a solid can potentially form or not.

The saturation index with respect to a solid can be expressed as $\log(IAP/K_{SO})$. The ion activity product IAP is calculated from activities derived from the concentrations determined in the solution. A positive saturation index implies oversaturation and thus the possibility that this phase can precipitate. A negative value means undersaturation with regard to the respective solid indicating that this solid is not stable in equilibrium with such a solution. As the use of saturation indices can be misleading when comparing phases which dissociate into a different number of ions, “effective” saturation indices can be calculated by dividing the saturation indices by the number of ions participating in the reactions to form the solids; i.e., the saturation indices for gypsum, portlandite,

Table 2 Measured concentrations in the pore solutions of an ordinary Portland cement (w/c = 0.4) hydrated for 69 days

Pressure (MPa)	Li (mmol/l)	Na (mmol/l)	K (mmol/l)	Ca (mmol/l)	Sr (mmol/l)	Al (mmol/l)	Si (mmol/l)	S (mmol/l)	OH (mmol/l) ^a	pH	C.B. ^b (%)
60–120	0.69	46	450	1.8	0.046	0.09	0.21	8.2	490	13.6	0
120–150	0.69	49	480	2.0	0.050	0.09	0.21	9.2	490	13.6	5
150–180	0.69	49	480	2.0	0.050	0.09	0.23	10	490	13.6	5
180–270	0.69	50	490	2.0	0.050	0.09	0.24	12	490	13.6	7
270–330	0.63	50	480	1.9	0.050	0.09	0.26	13	500	13.6	1

Details on the extraction procedure and the composition of the cement given in [17, 152]

^a The values for OH⁻ refer to free concentrations, all other values represent total concentrations

^b The charge balance error C.B. gives the surplus of cations (cations–anions), relative to the total charge caused theoretically by cations (i.e., [Na⁺] + [K⁺] + 2[Ca²⁺])



ettringite or monosulfate are divided by 2, 3, 15 or 11, respectively.

During the first hours of the hydration of Portland cements, the pore solutions are oversaturated with respect to gypsum, portlandite, ettringite, monosulfate and C-S-H ([7–10, 15, 100, 111, 124, 125, 153], Fig. 2). In cements containing relatively high fractions of potassium, also saturation with respect to syngenite has been observed [8, 111]. The agreement between the solid hydrate assemblage predicted by thermodynamic calculation based on the measured composition of the pore solution and the experimentally observed hydrate assemblage [8–10, 100, 154] is very good and emphasizes the relevance of the pore solution analysis for the processes observed in the solid phases.

The effective saturation indices for portlandite, gypsum, ettringite and monosulfate as given in Fig. 2 are similar to the values found in different studies [7–9, 17, 100, 125]. The kinetic of the precipitation of solids depends on the degree of oversaturation with respect to these phases but also on a number of other factors like the presence of surface defects, the composition of the solution, the presence of ions which hinder the reaction, and temperature [37, 39, 101, 102]. In highly oversaturated solutions, precipitation can be relatively fast; the precipitation rate decreases as the degree of oversaturation decreases until thermodynamic equilibrium is reached [37, 39, 155]. During the first hours of hydration many solids—i.e., alkali and calcium sulfates, free lime and, more slowly, also the clinker phases—dissolve and release ions into the pore solution. Thus, a certain degree of oversaturation with respect to precipitating solids is expected during the first day of cement hydration, which is in agreement with the experimental data. Some authors [7, 8, 100, 124, 156] observed that low-alkali cements exhibit a slightly lower degree of oversaturation with respect to portlandite and ettringite than Portland cements containing high alkali concentrations. As the growth rate of different solids decreases with increasing ionic strength [157, 158], such a slower precipitation rate at higher ionic strength would be consistent with a higher degree of oversaturation at higher alkali concentrations.

Although initially the calculated effective saturation indices with respect to ettringite in the pore solution of Portland cements are relatively high

(Fig. 2), they decrease after several hours when all gypsum and/or anhydrite is consumed. It has often been observed that the pore solutions of aged Portland cement pastes remain slightly oversaturated with respect to portlandite and ettringite [7–9, 17, 100, 125], but the source of this apparent oversaturation is unclear. Oversaturation can result from kinetic restraint for the formation of a solid. At higher temperature such kinetic restraint are more easily overcome. The decreasing levels of ettringite oversaturation with increasing temperatures (Fig. 2; [10, 125]) would be consistent with a kinetic restraint on ettringite formation.

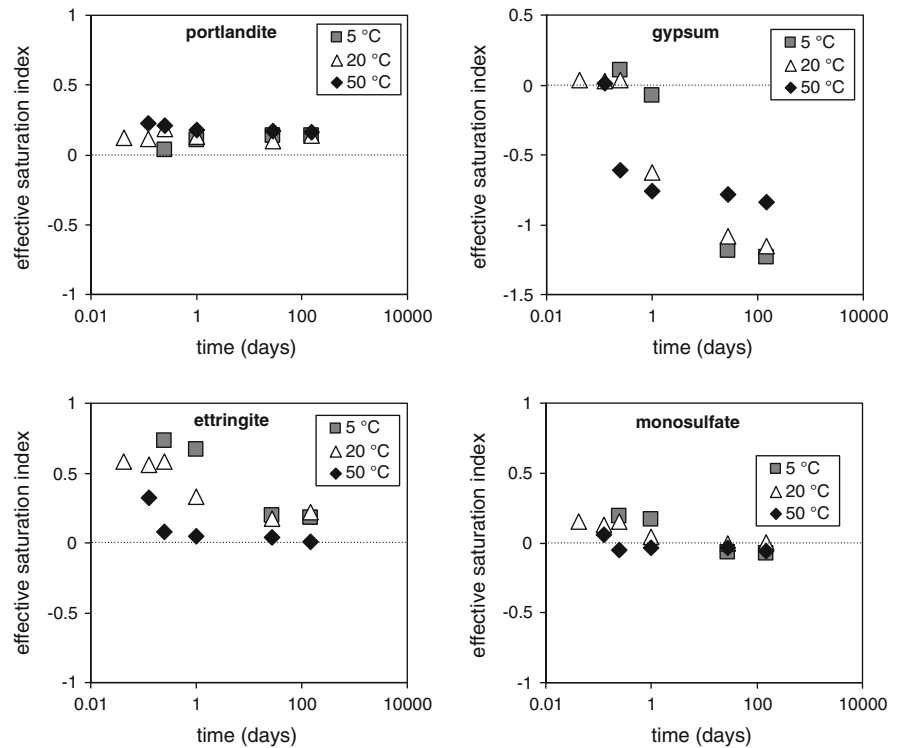
6.2 Modeling of hydrated systems

Thermodynamic modeling may also be used to calculate the stable phase assemblage assuming complete hydration of the starting materials. Changes in the overall chemical composition of a system or a different temperature do affect the amount as well as the kind of solid phases present. The simplest way to calculate the composition of a hydrated cement is to do simple mass balance calculations based on the chemical composition of the unhydrated cement [12, 14]. These calculations have the advantage that they can be carried out simply with a calculator, but also the disadvantage that the possible stable phase assemblage has to be known a priori. In well-defined systems as, e.g., ordinary Portland cements hydrated at ambient temperatures, a good agreement between these simple calculations and experimental results has been found [12, 14].

The use of thermodynamic calculations allows easy and fast parameter variations and thus the systematic study of the effects of changes in the composition of the starting materials or in temperature. Some examples of studies involving parameter variations are summarized in the following:

- In the presence of calcite, the stable phase assemblage in hydrated Portland cement includes, besides C-S-H, portlandite, ettringite, and hydro-talcite, also monocarbonate [9, 12, 13, 159–161]. It has been shown, both experimentally as well as by thermodynamic modeling that the presence of up to 5% of calcite reduces the porosity of hydrated cements and can increase the compressive strength [162]. In the presence of excess calcite,

Fig. 2 “Effective” saturation indices as a function of hydration time and temperature. A saturation index of 0 indicates equilibrium between liquid and solid; a value >0 indicates oversaturation and <0 indicates undersaturation. Measured data from [126]



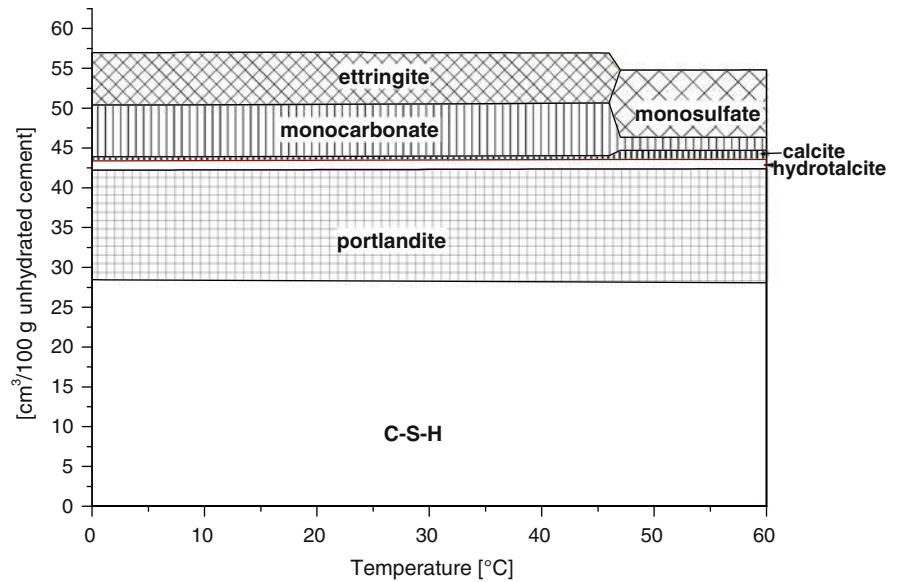
monocarbonate instead of monosulfate is stable which leads also to a stabilization of ettringite and thus to higher volume of the hydrated cement [9, 13].

- In the temperature range 0–47°C, thermodynamic modeling predicts for the Portland cement containing calcite, as main hydration products C-S-H, portlandite, monocarbonate and ettringite (see Fig. 3, [10, 57]). Above 48°C, ettringite and monocarbonate are predicted to be less stable than monosulfate: $\text{Ca}_6\text{Al}_2(\text{SO}_4)_3(\text{OH})_{12}\cdot 26\text{H}_2\text{O} + 2[3\text{CaO}\cdot\text{Al}_2\text{O}_3\cdot\text{CaCO}_3\cdot 11\text{H}_2\text{O}] \Leftrightarrow 3[3\text{CaO}\cdot\text{Al}_2\text{O}_3\cdot\text{CaSO}_4\cdot 12\text{H}_2\text{O}] + 2\text{CaCO}_3 + 18\text{H}_2\text{O}$. The observed changes in the composition around 48°C agree well with experimental observations [126, 129].
- Thermodynamic calculations indicate that thaumasite can form already at relatively low dissolved sulfate concentrations but only after the available aluminum has precipitated as ettringite [12, 72, 163]. Bellmann and Stark [164] calculated that the presence of low C/S C-S-H and the absence of portlandite can prevent thaumasite formation. These findings could also be confirmed experimentally [165].

6.3 Coupling of thermodynamic modeling with hydration

Thermodynamic modeling can also be used to predict quantitatively the amount of hydrates formed during the hydration of Portland cement. When cement is brought into contact with water, rapidly soluble solids such as alkali sulfates or gypsum dissolve until equilibrium with the pore solution is reached. The clinker phases hydrate at various rates, continuously releasing Ca, Si, Al, Fe and hydroxide into the solution, which then precipitate as C-S-H, ettringite and other hydrate phases. Dissolution rates of the clinker phases can be used to determine the amount of Ca, Al, Fe, Si, and hydroxide into solution released and thus to control the precipitation rates of C-S-H, ettringite, and the other hydrates. By combining an empirical description of the dissolution of the clinker phases as a function of time with a thermodynamic model that assumes equilibrium between the solution and the hydrates, the amount of hydrates formed can be described as a function of time [9, 10, 15–18, 57, 100]. The changes in capillary porosity, composition of the solid and liquid phase [9, 10, 15–18, 57, 100]

Fig. 3 Calculated volume of solids in a hydrated cement paste as a function of temperature. Adapted from [57]



as a function of time, relative humidity, water/cement ratio and temperature are calculated based on

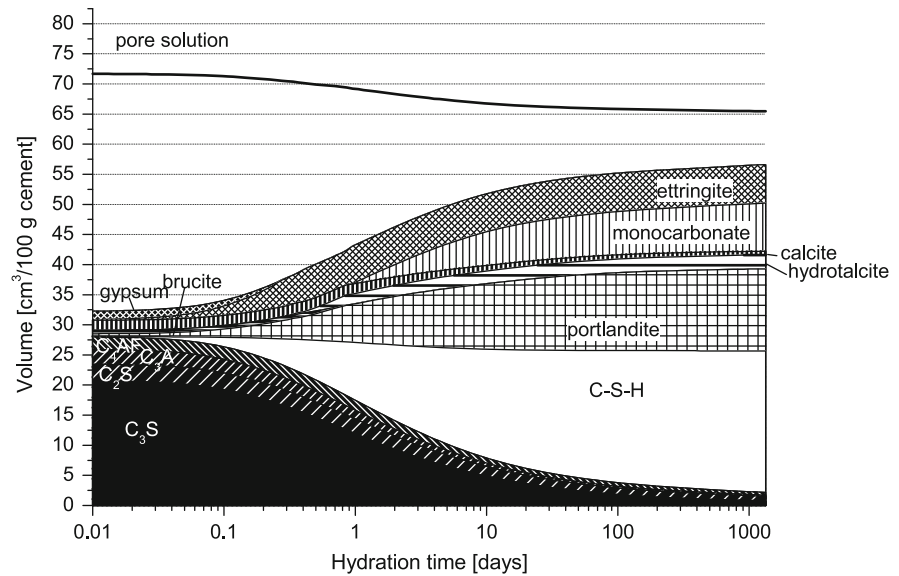
- (i) the composition of the cement paste,
- (ii) the calculated degree of dissolution of the clinkers and
- (iii) thermodynamic calculations using a consistent thermodynamic dataset.

Thermodynamic modeling, in combination with the calculated hydration rates, is able to predict the depletion of gypsum and/or anhydrite within the first day of hydration (Fig. 4). After a hydration time of approx. 1 day or less the precipitation of ettringite ceases as gypsum and/or anhydrite are exhausted; the calcium and sulfate concentrations in the pore solutions decrease strongly (Fig. 1). In calcite-containing cements, monocarbonate starts forming. Calcite is slowly consumed due to the formation of monocarbonate (Fig. 4). After hydration for half a year, it is predicted that the solid phases are C-S-H, portlandite, ettringite, monocarbonate, unhydrated clinker, hydrotalcite and calcite. With the exception of ettringite, the amount of each hydration product continues to slowly increase with time. At the same time the amount of pore solution and the capillary porosity decreases [10, 16, 18]. The total of the volume of the solid and liquid phase decreases during hydration (Fig. 4) as the water incorporated into the hydrates has a higher density than “free” water, leading to chemical shrinkage. The modeled changes of the composition of the solids and

liquid phase, of the enthalpy, of the porosity and the amount of pore solution during hydration have been found to agree well with the experimental data determined as a function of time (see e.g., Fig. 1; [9, 10, 15–18, 100]). The good agreement between experimental and modeled results indicates that the quasi equilibrium approach used in thermodynamic equilibrium calculations is valid for Portland cement systems.

The kind of solids predicted to precipitate in the different hydration studies depends on the original composition of the cement as well as on the completeness of the thermodynamic database used. For calcite-containing Portland cements the formation of C-S-H, portlandite, hydrotalcite, ettringite and monocarbonate is predicted, while in the absence of calcite the formation of monosulfate instead of monocarbonate and the presence of less ettringite is predicted [12, 13, 72, 154]. In past studies, generally calcite-free or calcite-poor cements were used [15, 16, 100]. Only recently, a critical evaluation of different experimental data combined with a set of new solubility measurements [43], could show that monosulfate is more stable than hydrogarnet in OPC systems, which agrees also with the experimental observations reported in the literature [9, 126, 160, 161, 166–168]. The continuing refinement of the available thermodynamic databases made and will continue to make thermodynamic predictions more and more precise.

Fig. 4 Calculated composition of a hydrating Portland cement as a function of time. Adapted from [9]



The alkalis originating from the dissolution of the alkali sulfates and of the clinker phases distribute between the aqueous solution and the precipitating C-S-H. As K and Na are the principal cations in the pore solution, their concentration controls the pH. Since the solubility of the cement minerals depend on pH, the modeling of alkali uptake by cementitious phases is of fundamental importance. In many cases empirical relations between the total amount of alkalis, the quantity of C-S-H and of pore solution have been used to estimate the uptake of alkali by C-S-H in hydrating cements [9, 15–17, 57, 75, 76, 78, 100].

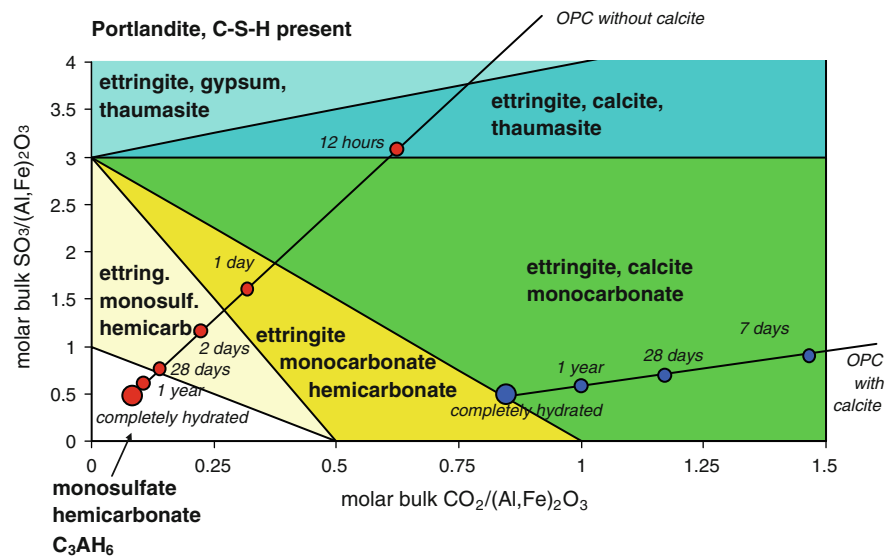
Thermodynamic modeling of the hydration can also help to visualize the changes that happen during the hydration of cements as well as their effect on the volume of the solids during hydration. This can be done by considering component ratios. In Fig. 5, the stable hydrate assemblage in an OPC system as a function of the fraction of carbonate and sulfate in the presence of excess C-S-H and portlandite is given. The stable hydrate assemblage depends on the molar fraction of carbonate and sulfate to aluminum (and iron). In hydrated, carbonate-poor systems, the formation of monosulfate and hemicarbonate can be expected. In many modern Portland cements, however, which contain calcite, the stable phase assemblage includes ettringite, monocarbonate and calcite [9, 12, 13, 159]. The fraction of carbonate and sulfate to aluminum (and iron) can change greatly during cement hydration, as the sulfate and carbonate

containing phases, such as alkali sulfates, gypsum or calcite, equilibrate relatively fast with the solution, while aluminum and iron are bound in the clinker phases and become available only very slowly. Thus, in a hydrating OPC initially a relatively high ratio of carbonate and sulfate to aluminum and iron is present (Fig. 5). During hydration, as the clinkers react, the effective molar ratio will decline as indicated in Fig. 5.

6.4 Coupled transport models

The same fundamental physical and chemical mechanisms apply to degradation and transport processes and they can be described using (quasi-)equilibrium calculations to describe the changes imposed by the environment as boundary conditions. Concrete interacting with its environment can undergo significant changes in its composition and in its microstructure. The transport of ions, gases or moisture in cementitious systems is affected by material properties such as porosity, tortuosity or the saturation state of the pores. These properties may also change during hydration due to chemical reactions. In addition the transport of ions is strongly affected by their interaction with cementitious systems, the precipitation of solids or the sorption of these ions on existing surfaces. Transport codes coupled with thermodynamic modeling are used to predict which hydrates are formed under which conditions, to assess their influence on the retention of different ions as well as

Fig. 5 Calculated phase assemblage of hydrating Portland cements. Adapted from [12, 169]. C-S-H and portlandite are always present, but not shown. The changes during the hydration of an OPC with 4% calcite and an OPC, where no additional calcite has been added (0.3% CO₂) [9], are indicated by dots



to take into account the influence of the formation of additional solids on the local porosity and thus on transport properties. Coupled transport can be used for the predictions of the long-term behavior and their durability in different environments [19–24]. A recent review of Glasser et al. [170] discusses in detail the mechanisms that govern transport in cementitious systems and different chemical degradation phenomena including chloride ingress, carbonation, decalcification and sulfate attack.

7 Concluding remarks and future challenges

Thermodynamic modeling in its different forms has been applied mainly to Portland cement systems. The approach, however, is equally valid for blended systems [29–31, 171] or for cementitious systems based on slags [139–141, 144]. The investigations of the processes and the composition of the hydrate assemblage in modern alternative cementing systems [172] will be a considerable challenge in the near future. The use of thermodynamic models, together with experimental investigations, is expected to further the development of new cementitious materials and blends significantly.

Thermodynamic modeling helps to deepen our understanding of the processes that govern cementitious systems, to interpret experimental observations and also to interpolate between investigated systems. Thermodynamic modeling, however, cannot replace

the experiments, as in many cases kinetic limitations cannot yet be predicted adequately and as for non Portland cement systems and blended systems important thermodynamic data are still missing. Thus, the results of thermodynamic modeling should, if possible, be verified against experimental data.

Thermodynamic modeling assumes a thermodynamic equilibrium. With regard to some solids, however, a metastable equilibrium will persist in many cementitious systems. Amorphous C-S-H is thermodynamically metastable with respect to crystalline phases. Similarly, AFm phases seem to be metastable with respect to siliceous hydrogarnets in the presence of silicate. Based on the experimental observations at room temperatures, these solids are generally not allowed to precipitate in thermodynamic calculations.

Alternatively to suppressing the formation of solids one might include both dissolution as well as precipitation kinetics in the thermodynamic calculations [89, 91, 155]. In such an approach the influence of the composition of the surrounding solution on both the kinetics of precipitation and dissolution can be taken into account individually. While for some pure systems, e.g. the C₃S–C–S–H–portlandite system, studies of dissolution and precipitation kinetics and the influence of some parameters are available [89, 91–93], these data are still missing for many parameters and most solids. Thus, at the moment the systematic application of kinetic models, which include the influence of the solution composition on both dissolution and precipitation kinetics, do not

seem to yet feasible. Such models would help greatly to improve our insight of the processes that govern cement hydration and might point towards options to optimize them.

In some systems, however, calculations are hampered by the lack of knowledge of thermodynamic properties, especially the ability of C-S-H at low C/S ratio to take up other ions such as aluminum, alkalis or sulfate is not well investigated. As the results of thermodynamic calculations can only be as reliable and complete as the underlying thermodynamic database, the measurement, collection as well as the critical assessment of thermodynamic data will have to be continued.

Not only reliable data for some solids are still missing, but also the influence of different parameters has not been included up to now in thermodynamic calculations. While thermodynamic data in the range of 0–100°C are available for many solids in cementitious systems, data on the combination of pressure and high temperature on the solubility of the different hydrates are not yet available.

Experimental determinations of the solubility of solids are carried out in the presence of excess water, while the relative humidity in hydrating cement can be reduced significantly, especially if low w/c ratios are employed or if the system is exposed to drying conditions. The reduction of the water content in many hydrates such as in ettringite, monosulfate, C_4AH_9 or C-S-H at lower relative humidity is generally not taken into account in thermodynamic calculations. In addition, a low relative humidity can also stabilize other solids; anhydrite becomes more stable than gypsum at low relative humidity and also monosulfate seems to become stabilized with regard to ettringite at lower relative humidities [173].

Acknowledgments Many thanks to Dmitrii Kulik, who helped me over many years to master GEMS, to Thomas Matschei and Göril Möschner, who worked hard to improve the cement thermodynamic databases and to Urs Berner, Fred Glasser, and Erich Wieland who offered many insights in applications of thermodynamics to cementitious systems. Thanks also to Frank Winnefeld, Ken Snyder, and Pietro Lura, whose comments helped to improve this manuscript.

References

1. Parkhurst DJ, Appelo CAJ (1999) User's Guide to PHREEQC (version 2): a computer program for speciation, batch reaction, one dimensional transport, and inverse geochemical calculations, in Water-Resources Investigation Report, Denver, Colorado
2. Westall JC, Zachary JL, Morel FMM (1976) MINEQL. Department of Civil Engineering, MIT, Cambridge, MA
3. Wolery TJ (1992) EQ3/6, A software package for geochemical modeling of aqueous systems: package overview and installation guide (version 7). Lawrence Livermore National Laboratory, Livermore, CA
4. van der Lee J, De Windt L (2002) CHESS tutorial and cookbook. Updated for version 3.0. Ecole Nationale Supérieure des Mines de Paris, Paris
5. Kulik D, Berner U, Curti E (2004) Modelling geochemical equilibrium partitioning with the GEMS-PSI Code. In: Smith B, Gschwend B (eds) PSI Scientific Report 2003/vol IV. Nuclear energy and safety. Paul Scherrer Institute, Villigen, Switzerland
6. Kulik D (2007) GEMS-PSI 2.2, available at <http://gems.web.psi.ch/>. PSI, Villigen, Switzerland
7. Rothstein D, Thomas JJ, Christensen BJ, Jennings HM (2002) Solubility behavior of Ca-, S-, Al-, and Si-bearing solid phases in Portland cement pore solutions as a function of hydration time. *Cem Concr Res* 32(10):1663–1671
8. Stark J, Möser B, Bellmann F (2007) Quantitative characterization of cement hydration. In: Setzer M (eds) Proceedings of the 5th International Essen Workshop, Transport in Concrete: nano- to macrostructure. Essen, Germany, Aedification Publishers, Freiburg June 11–13, pp 161–179
9. Lothenbach B, Le Saout G, Gallucci E, Scrivener K (2008) Influence of limestone on the hydration of Portland cements. *Cem Concr Res* 38(6):848–860
10. Lothenbach B, Matschei T, Möschner G, Glasser FP (2008) Thermodynamic modelling of the effect of temperature on the hydration and porosity of Portland cement. *Cem Concr Res* 38(1):1–18
11. Atkins M, Glasser FP, Moron IP, Jack JJ (1993) Thermodynamic modelling of blended cements at elevated temperature (50–90°C). DOE report DoE/HIMP/RR/94.011
12. Juel I, Herfort D, Gollop R, Konnerup-Madsen J, Jakobsen HJ, Skibsted J (2003) A thermodynamic model for predicting the stability of thaumasite. *Cem Conc Comp* 25:867–872
13. Matschei T, Lothenbach B, Glasser FP (2007) The role of calcium carbonate in cement hydration. *Cem Concr Res* 37(4):551–558
14. Nielsen EP, Herfort D, Geiker MR (2005) Phase equilibria of hydrated Portland cement. *Cem Concr Res* 35:109–115
15. Reardon EJ (1992) Problems and approaches to the prediction of the chemical composition in cement/water systems. *Waste Manag* 12:221–239
16. Lee JH, Roy DM, Mann B, Stahl D (1995) Integrated approach to modeling long-term durability of concrete engineered barriers in LLRW disposal facility. *Mat Res Soc Symp Proc* 353:881–889
17. Lothenbach B, Winnefeld F (2006) Thermodynamic modelling of the hydration of Portland cement. *Cem Concr Res* 36(2):209–226



18. Guillon E, Chen J, Chanvillard G (2008) Physical & chemical modeling of the hydration kinetics of OPC paste using a semi-analytical approach. In: Schlangen E, De Schutter G (eds) Proceedings of the International RILEM symposium on Concrete Modelling: CONMOD'08, 26–28 May 2008. RILEM Publications, Delft, The Netherlands, pp 165–172
19. Samson E, Marchand J, Beaudoin JJ (2000) Modeling the influence of chemical reactions on the mechanisms of ionic transport in porous materials: an overview. *Cem Concr Res* 30:1895–1902
20. Marchand J, Samson E, Maltais Y, Beaudoin JJ (2002) Theoretical analysis of the effect of weak sodium sulfate solutions on the durability of concrete. *Cem Conc Comp* 24(3–4):317–329
21. Maltais Y, Samson E, Marchand J (2004) Predicting the durability of Portland cement systems in aggressive environments-laboratory validation. *Cem Concr Res* 34(9):1579–1589
22. van der Lee J, De Windt L, Lagneau V (2008) Application of reactive transport models in cement-based porous media. In: Schlangen E, De Schutter G (eds) Proceedings of the International RILEM symposium on Concrete Modelling: CONMOD'08, 26–28 May 2008. RILEM Publications, Delft, The Netherlands, pp 463–470
23. Barbarulo R (2008) Modeling chemical degradations of cement pastes in contact with aggressive solutions: leaching and carbonation. In: Schlangen E, De Schutter G (eds) Proceedings of the International RILEM symposium on Concrete Modelling: CONMOD'08, 26–28 May 2008. RILEM Publications, Delft, The Netherlands, pp 213–223
24. Neuville N, Lecolier E, Aouad G, Damidot D (2008) Characterisation and modelling of physico-chemical degradation of cement-based materials used in oil wells. In: Schlangen E, De Schutter G (eds) Proc International RILEM symposium on Concrete Modelling: CONMOD'08, 26–28 May 2008. RILEM Publications, Delft, The Netherlands, pp 191–198
25. Berner UR (1987) Modelling porewater chemistry in hydrated Portland cement. *Mat Res Soc Symp Proc* 84:319–330
26. Glasser FP (1988) Modelling approach to the prediction of equilibrium phase distribution in slag-cement belnds and their solubility properties. *Mat Res Soc Symp Proc* 112:3–12
27. Reardon EJ (1990) An ion interaction model for the determination of chemical equilibria in cement/water systems. *Cem Concr Res* 20:175–192
28. Berner U (1990) A thermodynamic description of the evolution of pore water chemistry and uranium speciation during degradation of cement. PSI, Villigen, Switzerland
29. Atkins M, Bennett DG, Dawes AC, Glasser FP, Kindness A, Read D (1992) A thermodynamic model for blended cements. *Cem Concr Res* 22(2–3):497–502
30. Atkins M, Glasser FP, Kindness A (1992) Cement hydrate phases: solubility at 25°C. *Cem Concr Res* 22:241–246
31. Bennett DG, Read D, Atkins M, Glasser FP (1992) A thermodynamic model for blended cements. II: Cement hydrate phases; thermodynamic values and modelling studies. *J Nucl Mater* 190:315–325
32. Damidot D, Glasser FP (1992) Thermodynamic investigation of the CaO–Al₂O₃–CaSO₄–H₂O system at 50°C and 85°C. *Cem Concr Res* 22:1179–1192
33. Damidot D, Stronach S, Kindness A, Atkins M, Glasser FP (1994) Thermodynamic investigation of the CaO–Al₂O₃–CaCO₃–H₂O closed system at 25°C and the influence of Na₂O. *Cem Concr Res* 24(3):563–572
34. Neall FB (1994) Modelling of the near-field chemistry of the SMA repository at the Wellenberg Site. PSI, Villigen, Switzerland
35. Damidot D, Glasser FP (1995) Investigation of the CaO–Al₂O₃–SiO₂–H₂O system at 25°C by thermodynamic calculations. *Cem Concr Res* 25(1):22–28
36. Jacques D (2008) Benchmarking of the cement model and detrimental chemical reactions including temperature dependent parameters, SCK–CEN, NIRAS-MP5-03-XX
37. Appelo CAJ, Postma D (1996) Geochemistry, groundwater and pollution. A.A. Balkema, Rotterdam
38. Anderson GM, Crerar DA (1993) Thermodynamics in geochemistry: the equilibrium model. Oxford University Press, Oxford
39. Stumm W, Morgan JJ (1996) Aquatic chemistry: chemical equilibria and rates in natural waters, 3rd edn. Environmental Science and Technology. Wiley, New York
40. Kulik D (2002) Gibbs energy minimization approach to modeling sorption equilibria at the mineral interface: thermodynamic relations for multi-site surface complexation. *Am J Sci* 302:227–279
41. Nordstrom DK, Munoz JL (1988) Geochemical thermodynamics. Blackwell, Boston
42. Perkins RB, Palmer CD (1999) Solubility of ettringite (Ca₆[Al(OH)₆]₂(SO₄)₃·26H₂O) at 5–75°C. *Geochim Cosmochim Ac* 63(13/14):1969–1980
43. Matschei T, Lothenbach B, Glasser FP (2007) Thermodynamic properties of Portland cement hydrates in the system CaO–Al₂O₃–SiO₂–CaSO₄–CaCO₃–H₂O. *Cem Concr Res* 37(10):1379–1410
44. Parkhurst DJ (1990) Ion-association models and mean activity coefficients of various salts. In: Melchior DC, Bassett RL (eds) Chemical modeling of aqueous systems II. ACS Symposium series 416. American Chemical Society, Washington, DC, pp 30–43
45. Helgeson HC, Kirkham DH, Flowers GC (1981) Theoretical prediction of the thermodynamic behaviour of aqueous electrolyte at high pressures and temperatures. IV. Calculation of activity coefficients, osmotic coefficients, and apparent molal and standard and relative molal properties to 600°C and 5 kb. *Am J Sci* 281(10):1249–1516
46. Grenthe I, Puidomenech I (1997) Modelling in aquatic chemistry. OECD Nuclear Chemistry, Paris, France
47. Pitzer KS (1991) Ion interaction approach: theory and data correlation. In: Pitzer KS (ed) Activity coefficients in electrolyte solutions. CRC Press, Boca Raton, pp 75–153
48. Viallis H, Faucon P, Petit JC, Nonat A (1999) Interactions between salts (NaCl, CsCl) and calcium-silicate hydrates (C-S-H). *J Phys Chem B* 103(25):5212–5219
49. Viallis-Terrisse H, Nonat A, Petit JC (2001) Zeta-potential study of calcium silicate hydrates interacting with alkaline cations. *J Colloid Interface Sci* 253(1):140–149

50. Barbarulo R, Peycelon H, Prene S (2003) Experimental study and modelling of sulfate sorption on calcium silicate hydrate. *Ann Chim Sci Mater* 1(Suppl):S5–S10
51. Wieland E, Tits J, Kunz D, Dähn R (2008) Strontium uptake by cementitious materials. *Environ Sci Technol* 42(2):403–409
52. Johannesson B, Yamada K, Nilsson L-O, Hosokawa Y (2007) Multi-species ionic diffusion in concrete with account to interaction between ions in the pore solution and the cement hydrates. *Mater Struct* 40:651–665
53. Hosokawa Y, Yamada K, Johannesson B, Nilsson L-O (2008) A development of a multi-species mass transport model considering thermodynamic phase equilibrium. In: Schlangen E, De Schutter G (eds) Proceedings of the International RILEM symposium on Concrete Modelling: CONMOD'08. PILEM Publications SARL, PRO 58, Delft, The Netherlands, pp 543–550
54. Labbez C, Nonat A, Pochard I, Jönsson B (2007) Experimental and theoretical evidence of overcharging calcium silicate hydrate. *J Colloid Interface Sci* 309(2):303–307
55. Kulik DA, Kersten M (2001) Aqueous solubility diagrams for cementitious waste stabilization systems: II, End-member stoichiometries of ideal calcium silicates hydrate solid solutions. *J Am Ceram Soc* 84(12):3017–3026
56. Macphee DE, Barnett SJ (2004) Solution properties of solids in the ettringite-thaumasite solid solution series. *Cem Concr Res* 34:1591–1598
57. Lothenbach B (2008) Thermodynamic modelling of the effect of temperature on the hydration of Portland cement. In: Schlangen E, De Schutter G (eds) Proceedings of the International RILEM symposium on Concrete Modelling: CONMOD'08, 26–28 May 2008. RILEM Publications, Delft, The Netherlands, pp 393–400
58. Möschner G, Lothenbach B, Ulrich A, Figi R, Kretschmar R (2009) Solid solution between Al-ettringite and Fe-ettringite ($\text{Ca}_6[\text{Al}_{1-x}\text{Fe}_x(\text{OH})_6]_2(\text{SO}_4)_3 \cdot 26\text{H}_2\text{O}$). *Cem Concr Res* 39:482–489
59. Bruno J, Bosbach D, Kulik D, Navrotsky A (2007) Chemical thermodynamics, vol 10. Chemical thermodynamics of solid solutions of interest in nuclear waste management. North-Holland/Elsevier, Amsterdam, The Netherlands
60. Curti E (1999) Coprecipitation of radionuclides with calcite: estimation of partition coefficients based on a review of laboratory investigations and geochemical data. *Appl Geochem* 14(4):433–445
61. Helgeson HC, Delany JM, Nesbitt HW, Bird DK (1978) Summary and critique of the thermodynamic properties of rock-forming minerals. *Am J Sci* 278-A:1–229
62. Babushkin VI, Matveyev GM, Mchedlov-Petrosyan OP (1985) Thermodynamics of silicates. Springer, Berlin
63. Johnson JW, Oelkers EH, Helgeson HC (1992) SUPCRT92: a software package for calculating the standard molal thermodynamic properties of minerals, gases, aqueous species, and reactions from 1 to 5000 bar and 0 to 1000°C. *Comput Geosci* 18(7):899–947
64. Robie RA, Hemingway BS (1995) Thermodynamic properties of minerals and related substances at 298.15 K and 1 bar (105 Pascals) pressure and at higher temperatures. *US Geol Surv Bull* 2131:461.
65. Shock EL, Sassani DC, Willis M, Sverjensky DA (1997) Inorganic species in geologic fluids: correlations among standard molal thermodynamic properties of aqueous ions and hydroxide complexes. *Geochim Cosmochim Acta* 61(5):907–950
66. Sverjensky DA, Shock EL, Helgeson HC (1997) Prediction of the thermodynamic properties of aqueous metal complexes to 1000°C and 5 kb. *Geochim Cosmochim Acta* 61(7):1359–1412
67. Hummel W, Berner U, Curti E, Pearson FJ, Thoenen T (2002) Nagra/PSI chemical thermodynamic data base 01/01. Universal Publishers/uPUBLISH.com, USA (also published as Nagra Technical Report NTB 02-16, Wettingen, Switzerland)
68. Babushkin VI, Matveev OP, Mchedlov-Petrosjan OP (1965) Thermodynamika silikatov. Strojizdat, Moskau
69. Nikushchenko VM, Khotimchenko VS, Rumyantsev PF, Kalinin AI (1973) Determination of the standard free energies of formation of calcium hydroxyaluminates. *Cem Concr Res* 3:625–632
70. Barret P, Brandie D, Beau D (1983) Calcium hydrocarboaluminate, carbonate, alumina gel and hydrated aluminates solubility diagram calculated in equilibrium with CO_2g and with Na_{aq}^+ ions. *Cem Concr Res* 13: 789–800
71. Bourbon X (2003) Chemical conceptual model for cement based materials, mineral phases and thermodynamic data, ANDRA Technical Report C.NT.ASCM.03.026.A
72. Schmidt T, Lothenbach B, Romer M, Scrivener KL, Rentsch D, Figi R (2008) A thermodynamic and experimental study of the conditions of thaumasite formation. *Cem Concr Res* 38(3):337–349
73. Möschner G, Lothenbach B, Rose J, Ulrich A, Figi R, Kretschmar R (2008) Solubility of Fe-ettringite ($\text{Ca}_6[\text{Fe}(\text{OH})_6]_2(\text{SO}_4)_3 \cdot 26\text{H}_2\text{O}$). *Geochim Cosmochim Acta* 72(1):1–18
74. Stade H (1989) On the reaction of C-S-H(di, poly) with alkali hydroxides. *Cem Concr Res* 19:802–810
75. Hong S-Y, Glasser FP (1999) Alkali binding in cement pastes. Part I. The C-S-H phase. *Cem Concr Res* 29: 1893–1903
76. Hong S-Y, Glasser FP (2002) Alkali sorption by C-S-H and C-A-S-H gels. Part II. Role of alumina. *Cem Concr Res* 32(7):1101–1111
77. Taylor HFW (1987) A method for predicting alkali ion concentrations in cement pore solutions. *Adv Cem Res* 1(1):5–17
78. Brouwers HJH, van Eijk RJ (2003) Alkali concentrations of pore solution in hydrating OPC. *Cem Concr Res* 33:191–196
79. Kulik D, Tits J, Wieland E (2007) Aqueous-solid solution model of strontium uptake in C-S-H phases'. *Geochim Cosmochim Acta* 71(12, Suppl 1):A530
80. Faucon P, Delagrave A, Petit JC, Richet C, Marchand J, Zanni H (1999) Aluminium incorporation in calcium silicate hydrates (C-S-H) depending on their Ca/Si ratio. *J Phys Chem B* 103:7796–7802

81. Matschei T, Skapa R, Lothenbach B, Glasser FP (2007) The distribution of sulfate in hydrated Portland cement paste. Proceedings of the 12th ICCG, Montreal, Canada, 9–12 July 2007, pp W1-05.2
82. Schwiete HE, Iwai T (1964) The behaviour of the ferritic phase in cement during hydration. *Zement-Kalk-Gips* 17:379–386
83. Gollop RS, Taylor HFW (1994) Microstructural and microanalytical studies of sulfate attack. II. Sulfate-resisting Portland cement: ferrite composition and hydration chemistry. *Cem Concr Res* 24(7):1347–1358
84. Paul M, Glasser FP (2000) Impact of prolonged warm (85 degrees C) moist cure on Portland cement paste. *Cem Concr Res* 30(12):1869–1877
85. Collier NC, Milestone NB, Hill J, Godfrey IH (2006) The disposal of radioactive ferric floc. *Waste Manage* 26(7):769–775
86. Taylor HFW (1997) *Cement chemistry*. Thomas Telford Publishing, London
87. Johnson CA, Glasser FP (2003) Hydrotalcite-like minerals ($M_2Al(OH)_6(CO_3)_{0.5} \cdot xH_2O$, where $M = Mg, Zn, Co, Ni$) in the environment: synthesis, characterisation and thermodynamic stability. *Clay Clay Miner* 51:1–8
88. Allada RK, Navrotsky A, Boerio-Goates J (2005) Thermochemistry of hydrotalcite-like phases in the $MgO-Al_2O_3-CO_2-H_2O$ system: a determination of enthalpy, entropy, and free energy. *Am Miner* 90(2–3):329–335
89. Garrault S, Finot E, Lesniewska E, Nonat A (2005) Study of C-S-H growth on C3S surface during its early hydration. *Mater Struct* 38:435–442
90. Garrault S, Nonat A (2001) Hydrated layer formation on tricalcium and dicalcium silicate surfaces: experimental study and numerical simulations. *Langmuir* 17:8131–8138
91. Bullard JW (2008) A determination of hydration mechanisms for tricalcium silicate using a kinetic cellular automaton model. *J Am Ceram Soc* 91(7):2088–2097
92. Damidot D, Bellmann F, Möser B, Sovoidnich T (2007) Investigation of the early dissolution behavior of C3S. In: Proceedings of the 12th ICCG, Montreal, Canada, 9–12 July 2007, pp W1-06.5
93. Minard H, Garrault S, Regnaud L, Nonat A (2007) Mechanisms and parameters controlling the tricalcium aluminate reactivity in the presence of gypsum. *Cem Concr Res* 37:1418–1426
94. Juilland P, Gallucci E, Flatt RJ, Scrivener K (2009) Mechanisms of hydration of cementitious materials at early age. In: Proceedings of the 17th Internationale Baustofftagung (ibausil), 23–26 September 2009, vol 1. Weimar, Germany, pp 1-0201–1-0206
95. Bishnoi S, Scrivener KL (2009) Studying nucleation and growth kinetics of alite hydration using [mu]jc. *Cem Concr Res* 39(10):849–860
96. Parrot LJ (1986) Modelling the development of microstructure. In: Henniker NH (ed) Proceedings of the Research on the manufacture and use of cements. Engineering Foundation, New York, pp 43–73
97. Wells LS, Clarke WF, McMurdie HF (1943) Study of the system $CaO-Al_2O_3-H_2O$ at temperature of 21 and 90°C. *J Res Nat Bur Stand* 30:367–409
98. Pepler RB, Wells LS (1954) The system of lime, alumina, and water from 50 to 250°C. *J Res Nat Bur Stand* 52(2):75–92
99. Jappy TG, Glasser FP (1991) Synthesis and stability of silica-substituted hydrogarnet $Ca_3Al_2Si_{3-x}O_{12-4x}(OH)_{4x}$. *Adv Cem Res* 4:1–8
100. Lothenbach B, Wieland E (2006) A thermodynamic approach to the hydration of sulphate-resisting Portland cement. *Waste Manag* 26(7):706–719
101. Schott J, Pokrovsky OS, Oelkers EH (2009) The link between mineral dissolution/precipitation kinetics and solution chemistry. In: Oelkers EH, Schott J (eds) Reviews in mineralogy and geochemistry, vol 70. Thermodynamics and kinetics of water-rock interaction. Mineralogical Society of America Geochemical Society, Chantilly, VA
102. Brantley SL (2008) Kinetics of mineral dissolution. In: Brantley SL, Kubicki JD, White AF (eds) Kinetics of rock-water interaction. Springer, New York
103. Chou L, Garrels RM, Wollast R (1989) Comparative study of the kinetics and mechanisms of dissolution of carbonate minerals. *Chem Geol* 78:269–282
104. Inskeep WP, Bloom PR (1985) An evaluation of rate equations for calcite precipitation kinetics at pCO_2 less than 0.01 atm and pH greater than 8. *Geochim Cosmochim Acta* 49:2165–2180
105. Kontrec J, Kralj D, Brecevic L (2002) Transformation of anhydrous calcium sulphate into calcium sulphate dihydrate in aqueous solutions. *J Cryst Growth* 240:203–211
106. Zhang J, Nancollas GH (1992) Influence of calcium/sulfate molar ratio on the growth rate of calcium sulfate dihydrate at constant supersaturation. *J Cryst Growth* 118:287–294
107. Barret P, Bertrandie D (1980) Courbe d'instabilité minimale dans une solution métastable de CA. 7th ICCG 3-V, pp 134–139
108. Fujii K, Kondo W, Ueno H (1986) Kinetics of hydration of monocalcium aluminate. *J Am Ceram Soc* 69(4):361–364
109. Bertrandie D, Barret P (1986) Hydration elementary interfacial steps of calcium aluminates as cement compounds. In: Proceedings of the 8th International Congress on the Chemistry of Cement, vol 3, Rio de Janeiro, pp 79–85
110. Damidot D (2007) Calculation of critically supersaturated domains with respect to ettringite in the $CaO-Al_2O_3-CaSO_4-H_2O$ system at 20°C. In: Proceedings of the 12th ICCG, Montreal, Canada, 9–12 July 2007, pp W1-05.5
111. Gartner EM, Tang FJ, Weiss SJ (1985) Saturation factors for calcium hydroxide and calcium sulfates in fresh Portland cement pastes. *J Am Ceram Soc* 68(12):667–673
112. Michaux M, Fletcher P, Vidick B (1989) Evolution at early hydration times of the chemical composition of liquid phase of oil-well cement pastes with and without additives. Part I. Additive free cement pastes. *Cem Concr Res* 19:443–456
113. Goldschmidt A (1982) About the hydration theory and the composition of the liquid phase of Portland cement. *Cem Concr Res* 12:743–746

114. Locher FW, Richartz W, Sprung S (1976) Erstarren von zement I: reaktion und gefügteentwicklung. *Zement-Kalk-Gips* 29(10):435–442
115. Vernet C, Démoulian E, Gourdin P, Hawthorn F (1980) Hydration kinetics of Portland cement. 7th ICCI II 219–224
116. Vernet C, Démoulian E, Gourdin P, Hawthorn F (1980) Kinetics of slag cements hydration. 7th ICCI III, pp 128–133
117. Locher FW, Richartz W, Sprung S, Rechenberg W (1983) Erstarren von zement IV: einfluss der lösungszusammensetzung. *Zement-Kalk-Gips* 36(4):224–231
118. Way SJ, Shayan A (1989) Early hydration of a Portland cement in water and sodium hydroxide solutions: composition of solutions and nature of solid phases. *Cem Concr Res* 19:759–769
119. Longuet P, Burglen L, Zelwer A (1973) La phase liquide du ciment hydraté. *Revue des Matériaux de Construction* 676:35–41
120. Barneyback RS, Diamond S (1981) Expression and analysis of pore fluids of hardened cement pastes and mortars. *Cem Concr Res* 11:279–285
121. Diamond S (1981) Effects of two Danish flyashes on alkali contents or pore solutions of cement-flyash pastes. *Cem Concr Res* 11:383–394
122. Gunkel P (1983) Die Zusammensetzung der flüssigen Phase erstarrender und erhärtender Zemente. *Beton-Informationen* 23(1):3–8
123. Diamond S, Ong S (1994) Effects of added alkali hydroxides in mix water on long-term SO_4^{2-} concentrations in pore solution. *Cem Concr Comp* 16(3): 219–226
124. Goñi S, Lorenzo MP, Guerrero A, Hernández MS (1996) Calcium hydroxide saturation factors in the pore solution of hydrated Portland cement fly ash pastes. *J Am Ceram Soc* 79(4):1041–1046
125. Thomas JJ, Rothstein D, Jennings HM, Christensen BJ (2003) Effect of hydration temperature on the solubility behavior of Ca-, S-, Al-, and Si-bearing solid phases in Portland cement pastes. *Cem Concr Res* 33(12):2037–2047
126. Lothenbach B, Winnefeld F, Alder C, Wieland E, Lunk P (2007) Effect of temperature on the pore solution, microstructure and hydration products of Portland cement pastes. *Cem Concr Res* 37(4):483–491
127. Schwarz W (1995) Novel cement matrices by accelerated hydration of the ferrite phase in Portland cement via chemical activation: kinetics and cementitious properties. *Adv Cem Bas Mat* 2:189–200
128. Wieker W, Bade T, Winkler A, Herr R (1991) On the composition of pore solutions squeezed from autoclaved cement pastes. In: Nonat A, Mutin JC (eds) Proceedings of the International RILEM workshop hydration setting Dijon, 3–5 July 1991. E & FN Spon, London, pp 125–135
129. Christensen AN, Jensen TR, Hanson JC (2004) Formation of ettringite, $\text{Ca}_6\text{Al}_2(\text{SO}_4)_3(\text{OH})_{12}\cdot 26\text{H}_2\text{O}$, AFt, and monosulfate, $\text{Ca}_4\text{Al}_2\text{O}_6(\text{SO}_4)\cdot 14\text{H}_2\text{O}$, AFm-14, in hydrothermal hydration of Portland cement and of calcium aluminum oxide–calcium sulfate dihydrate mixtures studied by in situ synchrotron X-ray powder diffraction. *J Solid State Chem* 177(6):1944–1951
130. Glasser FP, Luke K, Angus MJ (1988) Modification of cement pore fluid compositions by pozzolanic additives. *Cem Concr Res* 18(2):165–178
131. Lorenzo P, Goñi S, Hernandez S, Guerrero A (1996) Effect of fly ashes with high alkali content on the alkalinity of the pore solution of hydrated Portland cement paste. *J Am Ceram Soc* 79(2):470–474
132. Shehata MH, Thomas MDA, Bleszynski RF (1999) The effects of fly ash composition on the chemistry of the pore solution in hydrated cement pastes. *Cem Concr Res* 29(12):1915–1920
133. Shehata MH, Thomas MDA (2002) Use of ternary blends containing silica fume and fly ash to suppress expansion due to alkali-silica reaction in concrete. *Cem Concr Res* 32(3):341–349
134. Larbi JA, Fraay ALA, Bijen JMJM (1990) The chemistry of the pore fluid of silica fume-blended cement systems. *Cem Concr Res* 20:506–516
135. Rasheeduzzafar, Hussain ES (1991) Effect of microsilica and blast furnace slag on pore solution composition and alkali-silica reaction. *Cem Concr Comp* 13:219–225
136. Coleman NJ, Page CL (1997) Aspects of the pore solution chemistry of hydrated cement pastes containing metakaolin. *Cem Concr Res* 27(1):147–154
137. Tishmack JK, Olek J, Diamond S, Sahu S (2001) Characterization of pore solutions expressed from high-calcium fly-ash-water pastes. *Fuel* 80:815–819
138. Vernet C (1982) Comportement de l'ion S⁻ au cours de l'hydratation des ciments riche en laitier (CLK). *Silicates industriels* 47:85–89
139. Matschei T, Bellmann F, Stark J (2005) Hydration behaviour of sulphate-activated slag cements. *Adv Cem Res* 17(4):167–178
140. Gruskovnjak A, Lothenbach B, Winnefeld F, Figi R, Ko SC, Adler M, Mäder U (2008) Hydration mechanisms of supersulphated slag cement. *Cem Concr Res* 38:983–992
141. Song SJ, Jennings HM (1999) Pore solution chemistry of alkali-activated ground granulated blast-furnace slag. *Cem Concr Res* 29(2):159–170
142. Puertas F, Fernández-Jiménez A, Blanco-Varela MT (2004) Pore solution in alkali-activated slag cement pastes. Relation to the composition and structure of calcium silicate hydrate. *Cem Concr Res* 34(1):139–148
143. Gruskovnjak A, Lothenbach B, Holzer L, Figi R, Winnefeld F (2006) Hydration of alkali-activated slag: comparison with ordinary Portland cement. *Adv Cem Res* 18(3):119–128
144. Lothenbach B, Gruskovnjak A (2007) Hydration of alkali-activated slag: thermodynamic modelling. *Adv Cem Res* 19(2):81–92
145. Koyanagi K (1932) Hydration of aluminous cement. *Concrete* 40(8):40–46
146. Winnefeld F, Lothenbach B (2009) Hydration of calcium sulfoaluminate cements: experimental findings and thermodynamic modelling. *Cem Concr Res* (in press) doi: [10.1016/j.cemconres.2009.08.014](https://doi.org/10.1016/j.cemconres.2009.08.014)
147. Li GS, Walenta G, Gartner E (2007) Formation and hydration of low-CO₂ cements based on belite, calcium sulfoaluminate and calcium aluminoferrite. In: Proceedings of the 12th ICCI, Montreal, Canada, 9–12 July 2007, pp TH3-15.3

148. Chatterji S (1991) On the relevance of expressed liquid analysis to the chemical processes occurring in cement paste. *Cem Concr Res* 21:269–272
149. Duchesne J, Bérubé MA (1994) Evaluation of the validity of the pore solution expression method from hardened cement pastes and mortars. *Cem Concr Res* 24(3): 456–462
150. Tritthart J (1989) Chloride binding in cement—I. Investigations to determine the composition of pore water in hardened cement. *Cem Concr Res* 19(4):586–594
151. Bérubé MA, Tremblay C (2004) Chemistry of pore solution expressed under high pressure: influence of various parameters and comparison with the hot-water extraction method. In: Proceedings of the 12th International Conference on Alkali-Aggregate Reaction in Concrete, vol I, Beijing, China, October 15–19, pp 833–842
152. Lothenbach B, Winnefeld F, Figi R (2007) The influence of superplasticizers on the hydration of Portland cement. In: Proceedings of the 12th ICCS, Montreal, Canada, 9–12 July 2007, pp W1-5.03
153. Stark J, Möser B, Bellmann F, Rössler C (2006) Thermodynamische Modellierung der Hydratation von OPC. In: Zementhydratation QCD (eds) Proc 16. Internationale Baustofftagung (ibausil), Weimar, Germany, 20–22 September, Tagungsbericht Band 1, pp 1-0047–1-0066
154. Lothenbach B, Schmidt T, Romer M (2007) Influence of limestone additions on sulfate ingress. In: De Belie N (ed) Proc Workshop on performance of cement-based materials in aggressive aqueous environments: characterization, modelling, test methods and engineering aspects, Ghent, Belgium, Online version on www.rilem.net. PRO 057, E-ISBN: 978-2-35158-059-2, pp 49–56
155. Bullard JW (2007) A three-dimensional microstructural model of reactions and transport in aqueous mineral systems. *Model Simul Mater Sci Eng* 15:711–738
156. Ma W, Brown PW, Shi D (1992) Solubility of $\text{Ca}(\text{OH})_2$ and $\text{CaSO}_4 \cdot 2\text{H}_2\text{O}$ in the liquid paste from hardened cement paste. *Cem Concr Res* 22:531–540
157. Yeboah YD, Saeed MR, Lee AKK (1994) Kinetics of strontium sulfate precipitation from aqueous electrolyte solutions. *J Cryst Growth* 135:323–330
158. Knowles-Van Cappellen VL, Van Cappellen P, Tiller CL (1997) Probing the charge of reactive sites at the mineral-water interface: effect of ionic strength on crystal growth kinetics of fluorite. *Geochim Cosmochim Acta* 61(9): 1871–1877
159. Kuzel H-J, Pöllmann H (1991) Hydration of C_3A in the presence of $\text{Ca}(\text{OH})_2$, $\text{CaSO}_4 \cdot 2\text{H}_2\text{O}$ and CaCO_3 . *Cem Concr Res* 21:885–895
160. Kuzel H, Baier H (1996) Hydration of calcium aluminate cements in the presence of calcium carbonate. *Eur J Miner* 8:129–141
161. Bonavetti VL, Rahhal VF, Irassar EF (2001) Studies on the carboaluminate formation in limestone filler-blended cements. *Cem Concr Res* 31:853–859
162. Matschei T, Herfort D, Lothenbach B, Glasser FP (2007) Relationship of cement paste mineralogy to porosity and mechanical properties. In: Proc Conference on Modelling of Heterogeneous Materials, Prague, June 25–27
163. Damidot D, Barnett SJ, Glasser FP, Macphee DE (2004) Investigation of the $\text{CaO}-\text{Al}_2\text{O}_3-\text{SiO}_2-\text{CaSO}_4-\text{CaCO}_3-\text{H}_2\text{O}$ system at 25°C by thermodynamic calculation. *Adv Cem Res* 16(2):69–76
164. Bellmann F, Stark J (2007) Prevention of thaumasite formation in concrete exposed to sulphate attack. *Cem Concr Res* 37(8):1215–1222
165. Bellmann F, Stark J (2008) The role of calcium hydroxide in the formation of thaumasite. *Cem Concr Res* 38(10):1154–1161
166. Barker AP, Cory HP (1991) The early hydration of limestone-filled cements. In: Swamy RN (ed) Proc blended cements in construction. Elsevier, Sheffield, UK, pp 107–124
167. Ingram K, Polusny M, Daugherty K, Rowe W (1990) Carboaluminate reactions as influenced by limestone additions. In: Klieger P, Hooton RD (eds) Proc Carbonate Additions to Cement, vol 1064. American Society for Testing and Materials (ASTM STP), Philadelphia, PA, pp 14–23
168. Bensted J (1980) Some hydration investigations involving Portland cement-effect of calcium carbonate substitution of gypsum. *World Cem Technol* 11(8):395–406
169. Matschei T, Lothenbach B, Glasser FP (2007) The AFm phase in Portland cement. *Cem Concr Res* 37(2):118–130
170. Glasser FP, Marchand J, Samson E (2008) Durability of concrete: degradation phenomena involving detrimental chemical reactions. *Cem Concr Res* 38(2):226–246
171. Atkins M, Glasser FP, Kindness A (1991) Phase relation and solubility modelling in the $\text{CaO}-\text{SiO}_2-\text{Al}_2\text{O}_3-\text{MgO}-\text{SO}_3-\text{H}_2\text{O}$ system: for application to blended cements. *Mat Res Soc Symp Proc* 212:387–394
172. Gartner E (2004) Industrially interesting approaches to “low- CO_2 ” cements. *Cem Concr Res* 34:1489–1498
173. Albert B, Guy B, Damidot D (2006) Water chemical potential: a key parameter to determine the thermodynamic stability of some cement phases in concrete? *Cem Concr Res* 36:783–790